

## Supplementary Information

### Nascent chain dynamics and ribosome interactions within folded ribosome–nascent chain complexes observed by NMR spectroscopy

Charles Burridge, Christopher A. Waudby\*, Tomasz Włodarski, Anaïs M. E. Cassaignau, Lisa D. Cabrita and John Christodoulou\*

Department of Structural and Molecular Biology, University College London, London WC1E 6BT, UK.

\* Email: c.waudby@ucl.ac.uk, j.christodoulou@ucl.ac.uk

## Table of Contents

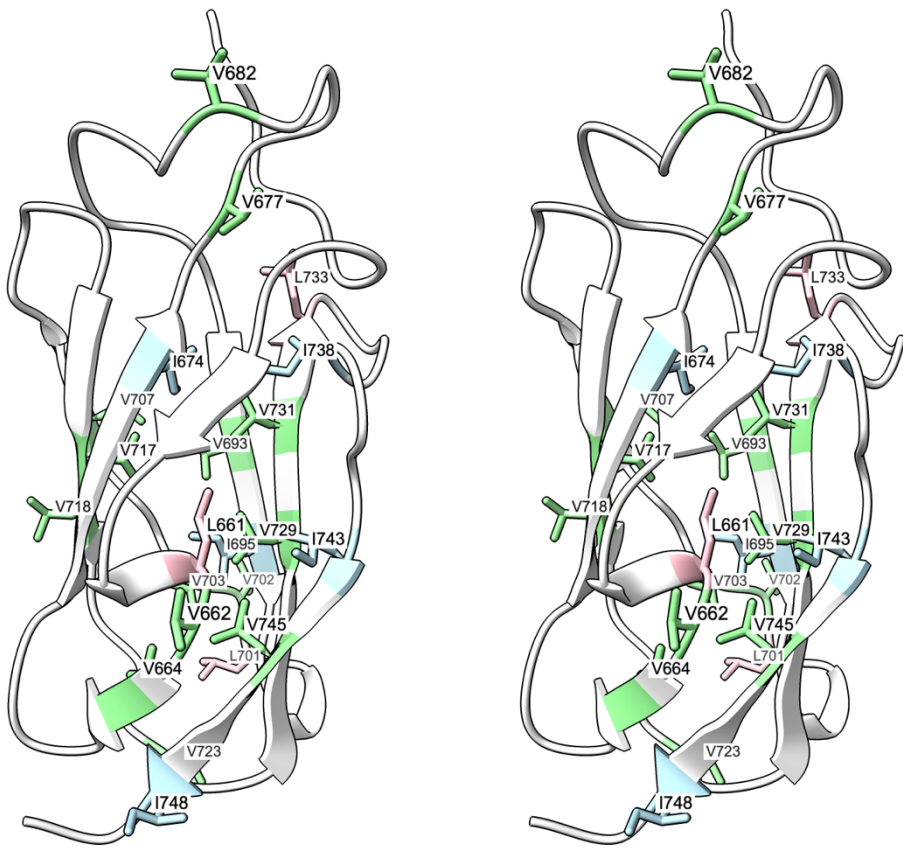
### Supplementary Figures

- Fig. S1 Annotated crystal structure of FLN5
- Fig. S2  $^1\text{H}, ^{13}\text{C}$  HMQC spectra of unoccupied 70S ribosomes and unlabeled isolated bL12
- Fig. S3 Pulse program for the measurement of methyl  $^1\text{H}$   $R_2$  relaxation rates
- Fig. S4 Time courses for quality control of RNC samples
- Fig. S5 Methyl  $^1\text{H}$   $R_2$  measurements for isolated FLN5 and FLN5+67 RNC
- Fig. S6 Correlation between  $^1\text{H}$   $R_2$  rates and  $S_{axis}^2 \tau_c$  values in isolated FLN5 vs glycerol
- Fig. S7 Correlation between  $S_{axis}^2 \tau_c$  values in isolated FLN5 and FLN5+67 RNC
- Fig. S8 Comparison of  $^1\text{H}, ^{13}\text{C}$  HMQC spectra of FLN5 wild-type, K2 and K5 variants.

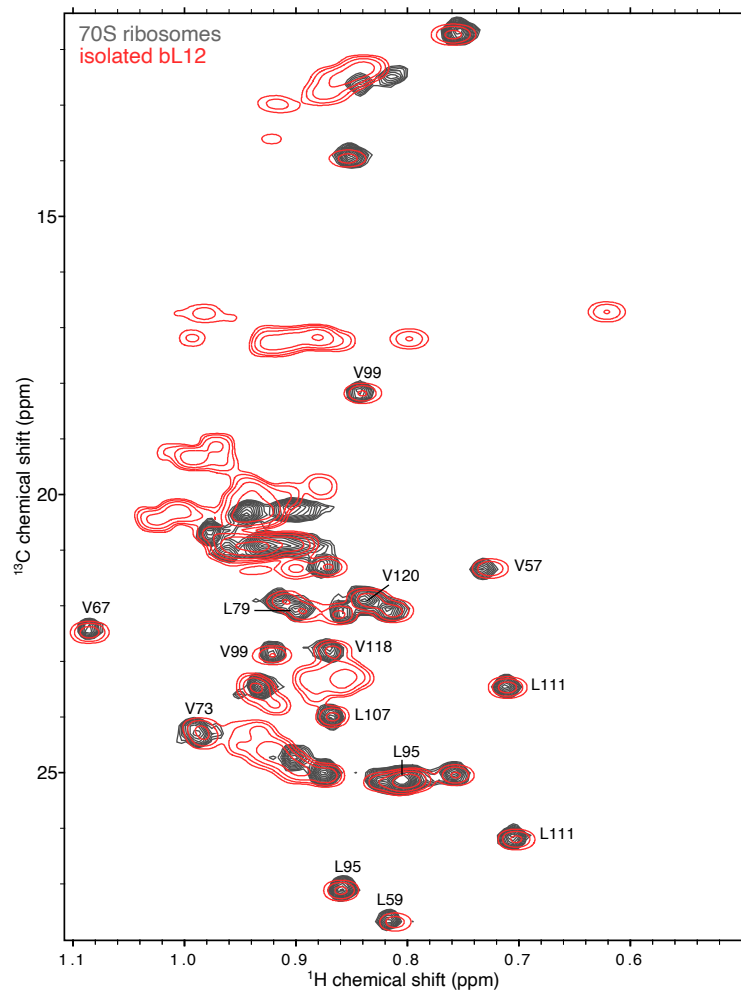
### Supplementary Tables

- Table S1 Protein sequences for nascent chains used in this study
- Table S2 Methyl  $^1\text{H}$   $R_2$  for isolated FLN5 vs glycerol concentration
- Table S3 Methyl  $S_{axis}^2 \tau_c$  values for isolated FLN5 vs glycerol concentration
- Table S4 Methyl  $^1\text{H}$   $R_2$  measurements for RNCs
- Table S5 Calculated methyl  $S_{axis}^2 \tau_c$  values for RNCs

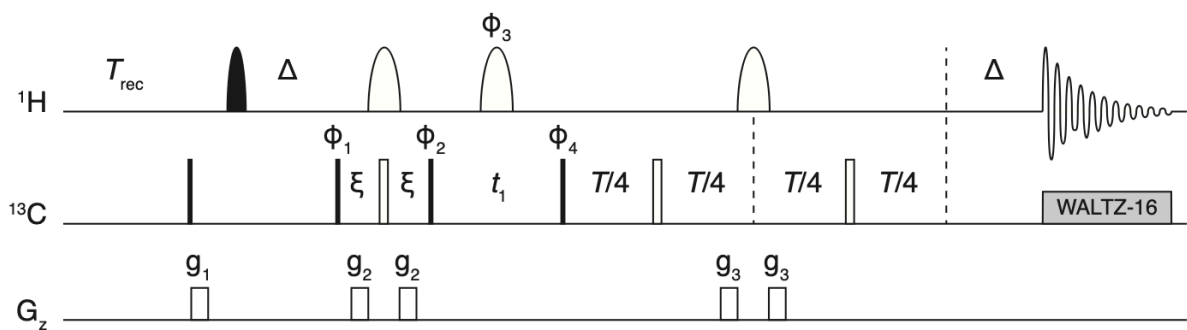
### References



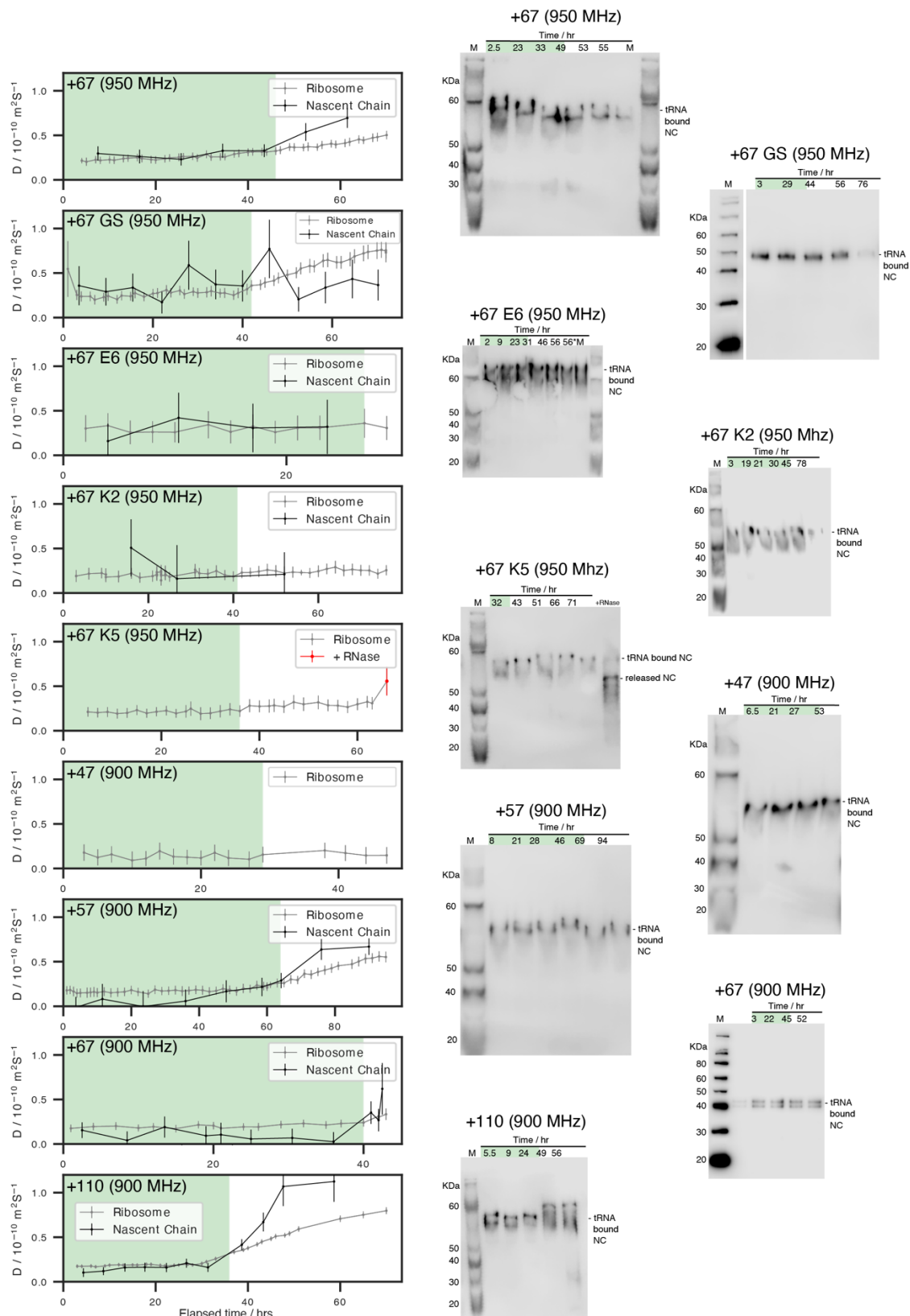
**Supplementary Figure 1:** Stereoview cartoon representation of the FLN5 crystal structure (pdb: 1qfh) showing the location of isoleucine, leucine and valine residues.



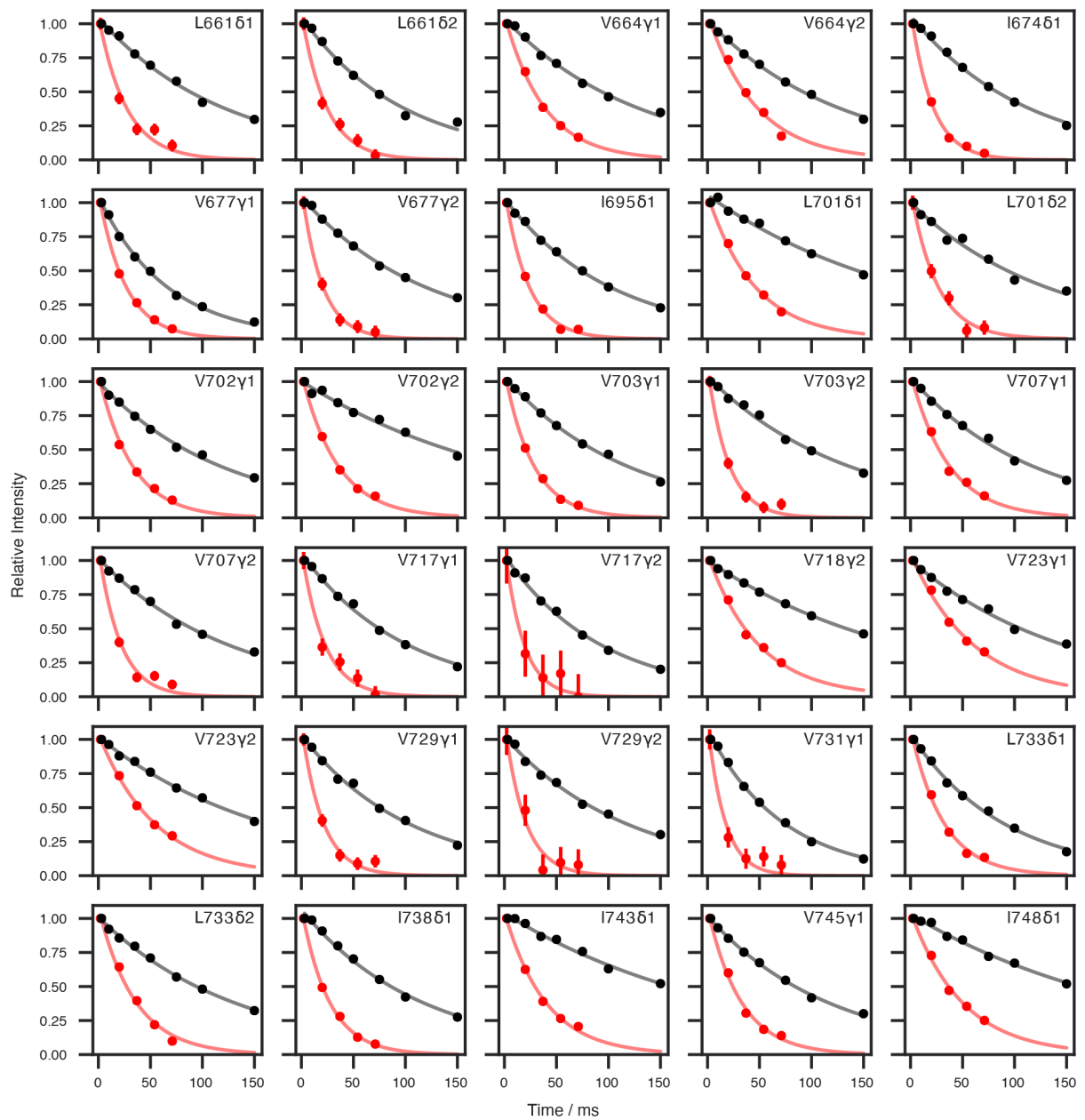
**Supplementary Figure 2:**  $^1\text{H},^{13}\text{C}$  HMQC spectra of ILV-labelled unoccupied 70S ribosomes (black, 298 K, 950 MHz) and unlabeled isolated bL12 (red, 298 K, 700 MHz).



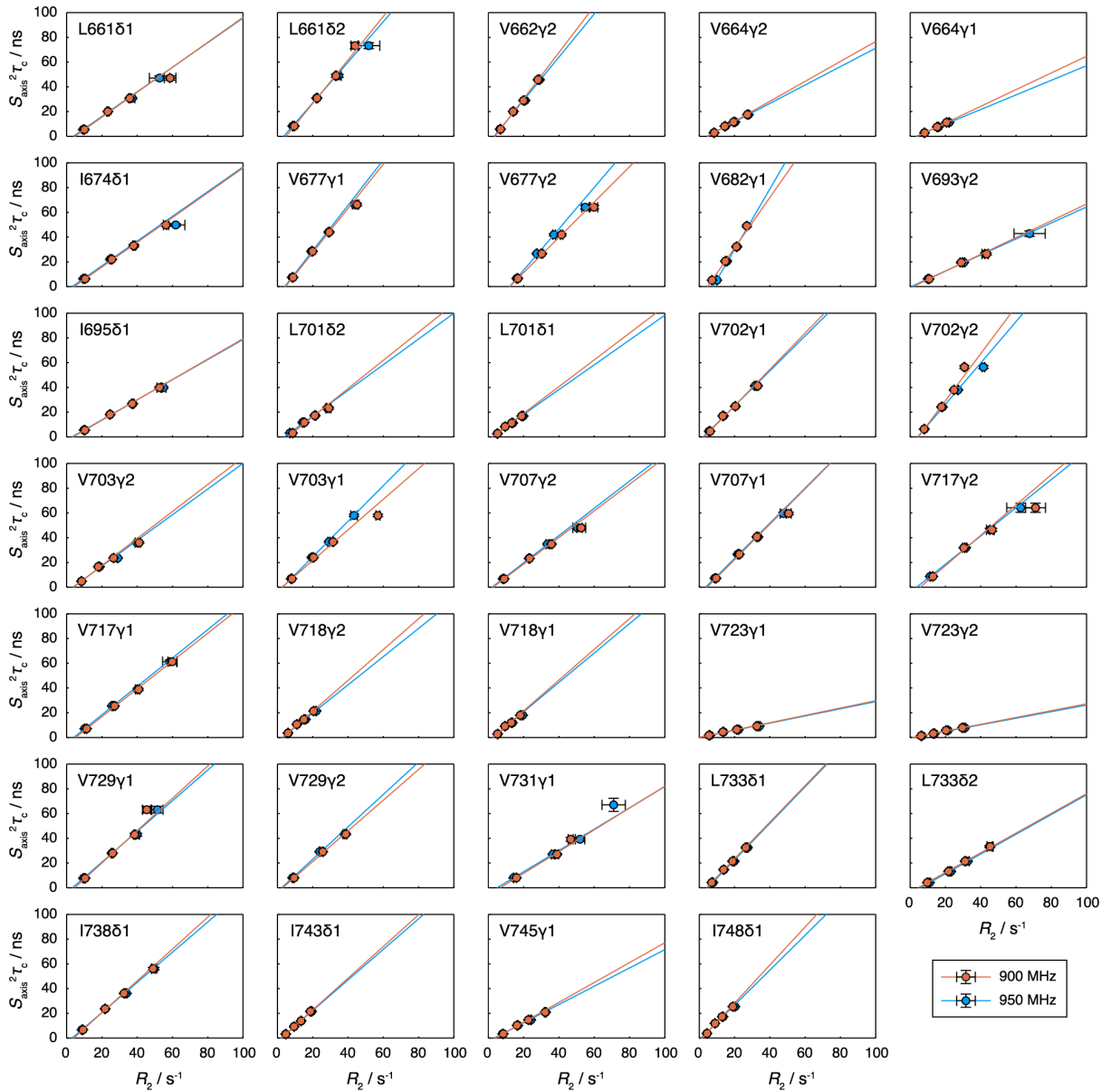
**Supplementary Figure 3:** Pulse program for the measurement of methyl  $^1\text{H}$   $R_2$  relaxation rates, based on a methyl SOFAST-HMQC experiment incorporating a filter for slowly relaxing inner transitions.  $T$  is the relaxation time,  $\Delta = 1/2J_{\text{CH}} = 4$  ms, and  $\xi = 1/8J_{\text{CH}} = 1$  ms.  $^1\text{H}$  shaped pulses were applied at 0.5 ppm; the solid pulse represents a  $120^\circ$  Pc9 excitation pulse (1120  $\mu\text{s}$  at 950 MHz) and the hollow pulse represents a  $180^\circ$  Rsnob pulse (564  $\mu\text{s}$  at 950 MHz). Phase cycles:  $\phi_1 = 0^\circ, 180^\circ$ ;  $\phi_2 = (0^\circ)_2, (180^\circ)_2$ ;  $\phi_3 = (0^\circ)_8, (120^\circ)_8, (240^\circ)_8$ ;  $\phi_4 = (0^\circ)_4, (180^\circ)_4$  and  $\phi_{\text{rx}} = 0^\circ, 180^\circ, 0^\circ, 180^\circ, 180^\circ, 0^\circ, 180^\circ, 0^\circ, 120^\circ, 300^\circ, 120^\circ, 300^\circ, 300^\circ, 120^\circ, 300^\circ, 120^\circ, 240^\circ, 60^\circ, 240^\circ, 60^\circ, 60^\circ, 240^\circ, 60^\circ, 240^\circ$ , with  $\phi_4$  incremented for States-TPPI quadrature detection. Gradient length, shape and power are:  $g_1 = 1$  ms (SMSQ10.100, 31%);  $g_2 = 50$   $\mu\text{s}$  (SINE.10, -40%);  $g_3 = 100$   $\mu\text{s}$  (SINE.10, 11%).



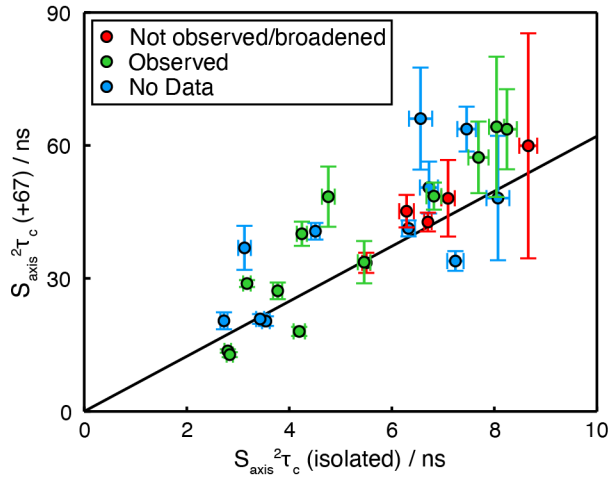
**Supplementary Figure 4: Time courses for quality control of RNC samples.** **(A)** Time course of nascent chain (I674, I738, I695 methyl resonances) and bL12 diffusion coefficients during data acquisition, shaded green area indicates measurement time used for analysis **(B)** Time course of nascent chain attachment by western blot (anti-histidine), using 2 pmol RNC aliquots taken periodically from a sample incubated in parallel with NMR data acquisition. The tRNA-bound nascent chain and released NC is indicated.



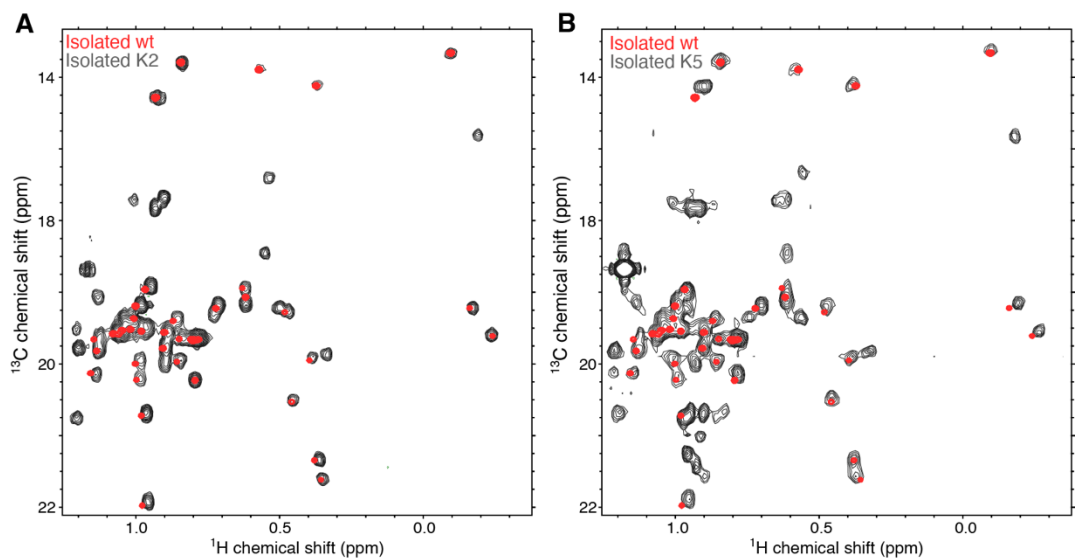
**Supplementary Figure 5:** Methyl  $^1\text{H}$   $\text{R}_2$  measurements for isolated FLN5 (black) and FLN5+67 RNC (red) (298 K, 950 MHz).



**Supplementary Figure 6:** Correlation between  ${}^1\text{H}$   $R_2$  rates and  $S_{\text{axis}}^2 \tau_c$  values for isoleucine, leucine and valine methyls in isolated FLN5 at varying concentrations of  $d_8$ -glycerol at 298 K, with  ${}^1\text{H}$   $R_2$  rates acquired at 900 MHz (orange) or 950 MHz (blue).



**Supplementary Figure 7:** Correlation between  $S_{\text{axis}}^2 \tau_c$  values measured for isolated FLN5, and  $S_{\text{axis}}^2 \tau_c$  values determined from  $^1\text{H}$  R<sub>2</sub> rates for the FLN5+67 RNC as shown in Fig. 2D, colored by observability of resonances previously reported for a uniformly  $^1\text{H}, ^{13}\text{C}$ -labelled FLN5 RNC<sup>1</sup>.



**Supplementary Figure 8:** Comparison of  $^1\text{H}, ^{13}\text{C}$  HMQC spectra of ILV-labelled FLN5 (298 K, 950 MHz) with isolated unlabeled (A) K2 FLN and (B) K5 FLN (298 K, 500 MHz).

Construct	Sequence
+47	MHHHHHHASKPAPSAEHSYAEGEGLVKVFDNAPAEFTIFAVDTKGVARTDGGDPFEVAINGPDGLVVDAKVTDDNNNDGTYG VVYDAPVEGNYNVNVTLRGNP1KNMP1DVKCIEGANGEDSSFGSFTFTVAAKNKKGEVKTYGGDKFEVSITGELFSTPVWIWWPRIRGPP
+57	MHHHHHHASKPAPSAEHSYAEGEGLVKVFDNAPAEFTIFAVDTKGVARTDGGDPFEVAINGPDGLVVDAKVTDDNNNDGTYG VVYDAPVEGNYNVNVTLRGNP1KNMP1DVKCIEGANGEDSSFGSFTFTVAAKNKKGEVKTYGGDKFEVSITGELFSTPVW IWWPRIRGPP
+67	MHHHHHHASKPAPSAEHSYAEGEGLVKVFDNAPAEFTIFAVDTKGVARTDGGDPFEVAINGPDGLVVDAKVTDDNNNDGTYG VVYDAPVEGNYNVNVTLRGNP1KNMP1DVKCIEGANGEDSSFGSFTFTVAAKNKKGEVKTYGGDKFEVSITGPAEEITLD AIELFSTPVWIWWPRIRGPP
+110	MHHHHHHASKPAPSAEHSYAEGEGLVKVFDNAPAEFTIFAVDTKGVARTDGGDPFEVAINGPDGLVVDAKVTDDNNNDGTYG VVYDAPVEGNYNVNVTLRGNP1KNMP1DVKCIEGANGEDSSFGSFTFTVAAKNKKGEVKTYGGDKFEVSITGPAEEITLD AIDNQDGTYTAAASLVGNGRFSTGVKLNGKHIEGSPFKQVLGNTSEFFSTPVWIWWPRIRGPP
+67 GS	MHHHHHHASKPAPSAEHSYAEGEGLVKVFDNAPAEFTIFAVDTKGVARTDGGDPFEVAINGPDGLVVDAKVTDDNNNDGTYG VVYDAPVEGNYNVNVTLRGNP1KNMP1DVKCIEGGGGSGGGSGGGSGGGSGGGSGGGSGGGSGGGSGGGSG GGELFSTPVWIWWPRIRGPP
+67 K2	MHHHHHHASKPAPSAEHSYAKGKGLVKVFDNAPAEFTIFAVDTKGVARTDGGDPFEVAINGPDGLVVDAKVTDDNNNDGTYG VVYDAPVEGNYNVNVTLRGNP1KNMP1DVKCIEGANGEDSSFGSFTFTVAAKNKKGEVKTYGGDKFEVSITGPAEEITLD AIELFSTPVWIWWPRIRGPP
+67 K5	MHHHHHHASKPAPSAEHSYAKGKGLVKVFDNAPAKFKIFAVDTKGVARTDGGDPFEVAINGPDGLVVKA KVTDDNNNDGTYG VVYDAPVEGNYNVNVTLRGNP1KNMP1DVKCIEGANGEDSSFGSFTFTVAAKNKKGEVKTYGGDKFEVSITGPAEEITLD AIELFSTPVWIWWPRIRGPP
+67 E6	MHHHHHHASKPAPSAEHSYAEGEGLVKVFDNAPAEFTIFAVDTKGVARTDGGDPFEVAINGPDGLVVDAKVTDDNNNDGTYG VVYDAPVEGNYNVEVTLEGEP1ENMPIEVECIEGANGEDSSFGSFTFTVAAKNKKGEVKTYGGDKFEVSITGPAEEITLD AIELFSTPVWIWWPRIRGPP

**Supplementary Table 1:** Protein sequences for nascent chains used in this study.

Methyl	0% 950 MHz	0% 900 MHz	40% 950 MHz	40% 900 MHz	50% 950 MHz	50% 900 MHz	60% 950 MHz	60% 900 MHz
L661δ1	8.6 ± 0.1	9.5 ± 0.1	22.2 ± 0.3	22.4 ± 0.4	34 ± 1	33.1 ± 0.5	51 ± 6	43 ± 2
L661δ2	9.3 ± 0.1	10.2 ± 0.1	23.5 ± 0.5	23.3 ± 0.6	37 ± 2	35.8 ± 0.7	52 ± 6	58 ± 3
V662γ2	6.59 ± 0.07	6.94 ± 0.06	14.27 ± 0.08	13.9 ± 0.1	20.8 ± 0.1	19.89 ± 0.06	29.0 ± 0.3	28.1 ± 0.3
V664γ1	8.24 ± 0.06	8.53 ± 0.06	14.84 ± 0.09	14.4 ± 0.1	20.3 ± 0.1	19.42 ± 0.06	27.9 ± 0.2	27.3 ± 0.3
V664γ2	8.03 ± 0.08	8.24 ± 0.07	16.1 ± 0.1	15.3 ± 0.1	22.1 ± 0.2	20.62 ± 0.09	-	-
I674δ1	9.52 ± 0.06	10.57 ± 0.07	24.7 ± 0.2	25.6 ± 0.3	38.3 ± 0.9	38.0 ± 0.4	61 ± 5	56 ± 2
V677γ1	16.1 ± 0.1	16.8 ± 0.2	27.5 ± 0.4	30.3 ± 0.5	37.2 ± 0.8	41.5 ± 0.6	54 ± 2	59 ± 2
V677γ2	8.28 ± 0.08	8.84 ± 0.07	19.2 ± 0.1	19.9 ± 0.2	29.0 ± 0.4	29.4 ± 0.2	43 ± 1	45 ± 1
V682γ1	10.0 ± 0.1	7.22 ± 0.06	15.66 ± 0.08	14.8 ± 0.1	21.4 ± 0.1	21.05 ± 0.06	-	27.0 ± 0.2
V693γ2	10.1 ± 0.1	10.8 ± 0.1	30.4 ± 0.6	28.9 ± 0.6	42 ± 2	43 ± 1	67 ± 9	-
I695δ1	9.83 ± 0.07	10.39 ± 0.06	24.6 ± 0.2	24.6 ± 0.3	37.6 ± 0.7	37.2 ± 0.3	54 ± 1	52 ± 1
L701δ1	5.09 ± 0.09	5.22 ± 0.05	9.49 ± 0.07	9.5 ± 0.07	13.9 ± 0.1	13.19 ± 0.04	19.8 ± 0.2	18.9 ± 0.2
L701δ2	7.1 ± 0.2	8.6 ± 0.2	14.3 ± 0.3	15.2 ± 0.3	21.4 ± 0.5	21.2 ± 0.2	28 ± 1	29 ± 1
V702γ1	8.13 ± 0.06	7.93 ± 0.06	18.4 ± 0.1	17.8 ± 0.2	27.1 ± 0.3	24.9 ± 0.1	41.5 ± 0.7	30.8 ± 0.3
V702γ2	5.54 ± 0.07	6.16 ± 0.05	13.77 ± 0.09	13.28 ± 0.09	20.5 ± 0.1	20.47 ± 0.07	31.7 ± 0.5	33.1 ± 0.4
V703γ1	8.34 ± 0.08	8.53 ± 0.07	18.7 ± 0.1	17.9 ± 0.2	28.9 ± 0.4	26.6 ± 0.2	39 ± 1	41.1 ± 0.9
V703γ2	7.66 ± 0.09	8.2 ± 0.08	19.4 ± 0.2	20.4 ± 0.3	29.2 ± 0.6	31.5 ± 0.3	43 ± 2	56 ± 1
V707γ1	8.79 ± 0.07	9.56 ± 0.08	21.8 ± 0.2	22.8 ± 0.3	33.3 ± 0.5	32.6 ± 0.3	47 ± 2	50 ± 1
V707γ2	8.23 ± 0.08	8.99 ± 0.09	23.1 ± 0.3	23.3 ± 0.4	33.5 ± 0.8	35.8 ± 0.5	50 ± 3	52 ± 2
V717γ1	10.22 ± 0.08	11.4 ± 0.1	25.8 ± 0.4	27.2 ± 0.4	40 ± 1	40.8 ± 0.6	58 ± 4	59 ± 2
V717γ2	11.3 ± 0.1	12.9 ± 0.1	31.5 ± 0.6	30.4 ± 0.7	45 ± 2	46 ± 1	62 ± 8	71 ± 6
V718γ1	6.05 ± 0.06	5.94 ± 0.04	11.06 ± 0.05	10.91 ± 0.05	15.9 ± 0.09	14.93 ± 0.03	21.9 ± 0.1	20.4 ± 0.2
V718γ2	5.34 ± 0.06	5.13 ± 0.03	9.44 ± 0.04	9.41 ± 0.04	13.67 ± 0.08	12.96 ± 0.02	19.4 ± 0.2	18.1 ± 0.1
V723γ1	6.67 ± 0.06	6.15 ± 0.04	13.8 ± 0.07	13.13 ± 0.07	21.4 ± 0.1	20.33 ± 0.06	31.0 ± 0.3	29.6 ± 0.3
V723γ2	6.06 ± 0.06	5.49 ± 0.03	13.8 ± 0.08	13.35 ± 0.08	22.3 ± 0.2	21.24 ± 0.07	34.1 ± 0.5	32.6 ± 0.4
V729γ1	9.51 ± 0.09	10.5 ± 0.1	25.6 ± 0.4	26.1 ± 0.5	39 ± 1	38.6 ± 0.6	51 ± 3	45 ± 2
V729γ2	8.52 ± 0.09	9.4 ± 0.1	23.9 ± 0.3	25.7 ± 0.5	38 ± 1	38.7 ± 0.6	-	-
V731γ1	14.3 ± 0.1	15.9 ± 0.1	36.5 ± 0.9	38.9 ± 0.9	51 ± 3	46 ± 1	71 ± 7	-
L733δ1	11.0 ± 0.2	9.7 ± 0.1	23.1 ± 0.4	21.7 ± 0.4	32.6 ± 0.9	31.1 ± 0.4	45 ± 1	45 ± 2
L733δ2	7.77 ± 0.09	7.05 ± 0.08	14.0 ± 0.1	13.8 ± 0.1	19.8 ± 0.2	18.86 ± 0.07	27.4 ± 0.3	26.4 ± 0.4
I738δ1	8.63 ± 0.05	9.3 ± 0.06	21.9 ± 0.1	21.8 ± 0.2	33.9 ± 0.4	32.6 ± 0.2	49 ± 1	49 ± 1
I743δ1	4.6 ± 0.05	4.73 ± 0.03	9.38 ± 0.05	9.4 ± 0.04	13.45 ± 0.09	13.31 ± 0.03	19.4 ± 0.2	18.6 ± 0.1
V745γ1	8.0 ± 0.06	8.46 ± 0.06	16.8 ± 0.1	16.2 ± 0.1	24.1 ± 0.3	22.65 ± 0.09	32.4 ± 0.4	32.2 ± 0.5
I748δ1	4.36 ± 0.05	4.43 ± 0.03	8.85 ± 0.03	8.94 ± 0.04	13.55 ± 0.07	12.9 ± 0.02	20.3 ± 0.1	19.0 ± 0.1

**Supplementary Table 2:** Methyl  $^1\text{H}$   $R_2$  for isolated FLN5 at glycerol concentrations of 0, 40, 50 and 60 % (w/w), acquired at 900 and 950 MHz, 298 K.

Methyl	0%	40%	50%	60%
L661 $\delta$ 1	8.2 $\pm$ 0.2	30.9 $\pm$ 0.4	48 $\pm$ 1	73 $\pm$ 2
L661 $\delta$ 2	5.5 $\pm$ 0.1	20.0 $\pm$ 0.3	30.8 $\pm$ 0.6	47 $\pm$ 2
V662 $\gamma$ 2	5.73 $\pm$ 0.09	20.0 $\pm$ 0.2	28.9 $\pm$ 0.3	45.8 $\pm$ 0.5
V664 $\gamma$ 1	2.84 $\pm$ 0.06	8.2 $\pm$ 0.1	11.5 $\pm$ 0.1	17.5 $\pm$ 0.2
V664 $\gamma$ 2	2.8 $\pm$ 0.06	7.52 $\pm$ 0.07	11.2 $\pm$ 0.2	19.2 $\pm$ 0.4
I674 $\delta$ 1	6.3 $\pm$ 0.1	22.1 $\pm$ 0.3	33.1 $\pm$ 0.9	49 $\pm$ 1
V677 $\gamma$ 1	6.6 $\pm$ 0.2	26.6 $\pm$ 0.4	42.0 $\pm$ 0.8	64 $\pm$ 1
V677 $\gamma$ 2	7.5 $\pm$ 0.2	28.5 $\pm$ 0.3	44.1 $\pm$ 0.6	66.3 $\pm$ 0.9
V682 $\gamma$ 1	5.19 $\pm$ 0.08	20.5 $\pm$ 0.3	32.2 $\pm$ 0.4	49.0 $\pm$ 0.8
V693 $\gamma$ 2	6.2 $\pm$ 0.1	19.5 $\pm$ 0.4	26.4 $\pm$ 0.8	42 $\pm$ 2
I695 $\delta$ 1	5.5 $\pm$ 0.08	18.1 $\pm$ 0.2	26.8 $\pm$ 0.3	39.8 $\pm$ 0.7
L701 $\delta$ 1	2.72 $\pm$ 0.07	8.34 $\pm$ 0.07	11.2 $\pm$ 0.1	16.9 $\pm$ 0.2
L701 $\delta$ 2	3.1 $\pm$ 0.1	11.7 $\pm$ 0.2	17.3 $\pm$ 0.4	23.2 $\pm$ 0.8
V702 $\gamma$ 1	6.3 $\pm$ 0.1	24.2 $\pm$ 0.2	38.0 $\pm$ 0.4	56 $\pm$ 1
V702 $\gamma$ 2	4.51 $\pm$ 0.08	16.9 $\pm$ 0.2	24.8 $\pm$ 0.3	41.3 $\pm$ 0.4
V703 $\gamma$ 1	4.8 $\pm$ 0.1	16.6 $\pm$ 0.2	23.6 $\pm$ 0.4	36.0 $\pm$ 0.7
V703 $\gamma$ 2	6.8 $\pm$ 0.1	24.0 $\pm$ 0.3	36.7 $\pm$ 0.7	58.0 $\pm$ 0.9
V707 $\gamma$ 1	7.2 $\pm$ 0.2	26.6 $\pm$ 0.3	40.7 $\pm$ 0.4	59 $\pm$ 1
V707 $\gamma$ 2	6.7 $\pm$ 0.2	23.3 $\pm$ 0.3	34.8 $\pm$ 0.6	47 $\pm$ 1
V717 $\gamma$ 1	7.1 $\pm$ 0.1	25.5 $\pm$ 0.3	38.9 $\pm$ 0.8	61 $\pm$ 1
V717 $\gamma$ 2	8.7 $\pm$ 0.2	31.9 $\pm$ 0.3	46 $\pm$ 1	64 $\pm$ 4
V718 $\gamma$ 1	3.54 $\pm$ 0.07	10.6 $\pm$ 0.1	14.6 $\pm$ 0.2	21.4 $\pm$ 0.2
V718 $\gamma$ 2	2.85 $\pm$ 0.04	9.12 $\pm$ 0.05	11.9 $\pm$ 0.1	18.0 $\pm$ 0.2
V723 $\gamma$ 1	1.36 $\pm$ 0.03	3.16 $\pm$ 0.08	5.8 $\pm$ 0.3	7.8 $\pm$ 0.1
V723 $\gamma$ 2	1.72 $\pm$ 0.03	4.47 $\pm$ 0.09	6.4 $\pm$ 0.2	9.1 $\pm$ 0.2
V729 $\gamma$ 1	7.7 $\pm$ 0.2	28.0 $\pm$ 0.3	42 $\pm$ 1	63 $\pm$ 3
V729 $\gamma$ 2	8.0 $\pm$ 0.1	29.1 $\pm$ 0.4	43.4 $\pm$ 0.6	63 $\pm$ 2
V731 $\gamma$ 1	8.1 $\pm$ 0.2	27.0 $\pm$ 0.5	39 $\pm$ 2	67 $\pm$ 5
L733 $\delta$ 1	4.2 $\pm$ 0.1	13.2 $\pm$ 0.2	21.5 $\pm$ 0.4	33.4 $\pm$ 0.7
L733 $\delta$ 2	4.2 $\pm$ 0.1	14.7 $\pm$ 0.2	21.5 $\pm$ 0.3	32.5 $\pm$ 0.5
I738 $\delta$ 1	6.7 $\pm$ 0.07	23.6 $\pm$ 0.2	36.2 $\pm$ 0.3	56 $\pm$ 1
I743 $\delta$ 1	3.17 $\pm$ 0.07	9.31 $\pm$ 0.04	13.9 $\pm$ 0.1	21.6 $\pm$ 0.2
V745 $\gamma$ 1	3.43 $\pm$ 0.08	10.3 $\pm$ 0.1	14.7 $\pm$ 0.2	20.9 $\pm$ 0.4
I748 $\delta$ 1	3.77 $\pm$ 0.09	11.85 $\pm$ 0.06	17.3 $\pm$ 0.1	25.4 $\pm$ 0.2

**Supplementary Table 3:** Methyl  $S_{axis}^2 \tau_c$  values for isolated FLN5 at glycerol concentrations of 0, 40, 50 and 60 % (w/w) recorded at 900 and 950 MHz, 298 K.

Methyl	$^1\text{H}$ $R_2$ ( $\text{s}^{-1}$ )								
	+67 950 MHz	+67 GS 950 MHz	+67 E6 950 MHz	+67 K2 950 MHz	+47 900 MHz	+57 900 MHz	+67 900 MHz	+110 900 MHz	
L661 $\delta$ 1	37.7 $\pm$ 4.7	35.0 $\pm$ 11.0	35.0 $\pm$ 8.1	-	-	70.2 $\pm$ 9.9	50.0 $\pm$ 7.2	37.3 $\pm$ 6.1	
L661 $\delta$ 2	42.3 $\pm$ 5.5	42.0 $\pm$ 11.0	49.0 $\pm$ 20.0	-	-	88.0 $\pm$ 18.0	41.7 $\pm$ 6.8	41.5 $\pm$ 7.1	
V664 $\gamma$ 1	26.4 $\pm$ 0.61	28.5 $\pm$ 2.3	28.0 $\pm$ 1.4	46.8 $\pm$ 6.5	46.6 $\pm$ 7.7	42.7 $\pm$ 2.3	27.2 $\pm$ 1.2	20.58 $\pm$ 0.61	
V664 $\gamma$ 2	21.54 $\pm$ 0.65	-	-	-	-	-	-	20.86 $\pm$ 0.69	
I674 $\delta$ 1	48.4 $\pm$ 3.3	45.5 $\pm$ 8.9	40.1 $\pm$ 5.3	-	-	57.3 $\pm$ 6.2	51.9 $\pm$ 4.6	35.5 $\pm$ 2.1	
V677 $\gamma$ 1	38.9 $\pm$ 2.5	43.4 $\pm$ 8.9	38.7 $\pm$ 2.8	-	-	58.0 $\pm$ 5.3	41.0 $\pm$ 5.9	36.6 $\pm$ 3.8	
V677 $\gamma$ 2	51.6 $\pm$ 6.7	-	42.0 $\pm$ 13.0	-	-	-	-	42.7 $\pm$ 6.4	
I695 $\delta$ 1	44.3 $\pm$ 2.5	55.7 $\pm$ 8.6	49.3 $\pm$ 6.2	146.0 $\pm$ 30.0	-	70.1 $\pm$ 6.1	45.7 $\pm$ 3.4	33.7 $\pm$ 1.8	
L701 $\delta$ 1	22.26 $\pm$ 0.76	21.1 $\pm$ 1.8	24.1 $\pm$ 2.9	82.0 $\pm$ 13.0	-	34.4 $\pm$ 2.3	20.8 $\pm$ 1.4	15.93 $\pm$ 0.62	
L701 $\delta$ 2	39.3 $\pm$ 4.1	43.0 $\pm$ 17.0	-	-	-	57.7 $\pm$ 9.9	37.1 $\pm$ 6.5	27.5 $\pm$ 2.2	
V702 $\gamma$ 1	31.0 $\pm$ 1.0	-	27.2 $\pm$ 1.2	-	39.8 $\pm$ 2.5	-	-	-	
V702 $\gamma$ 2	28.98 $\pm$ 0.74	29.3 $\pm$ 2.3	18.6 $\pm$ 1.5	84.0 $\pm$ 10.0	-	50.7 $\pm$ 1.7	37.73 $\pm$ 0.91	21.43 $\pm$ 0.83	
V703 $\gamma$ 1	36.7 $\pm$ 2.1	31.9 $\pm$ 5.3	31.3 $\pm$ 2.4	83.0 $\pm$ 20.0	-	52.6 $\pm$ 5.8	37.6 $\pm$ 3.4	29.1 $\pm$ 2.3	
V703 $\gamma$ 2	50.2 $\pm$ 5.7	49.0 $\pm$ 15.0	33.9 $\pm$ 3.2	-	-	70.8 $\pm$ 6.2	43.8 $\pm$ 8.7	31.1 $\pm$ 2.8	
V707 $\gamma$ 1	27.5 $\pm$ 1.5	27.4 $\pm$ 4.1	-	-	-	-	-	-	
V707 $\gamma$ 2	48.0 $\pm$ 5.2	35.4 $\pm$ 9.3	34.4 $\pm$ 3.7	-	-	-	-	-	
V717 $\gamma$ 1	45.9 $\pm$ 7.4	27.0 $\pm$ 18.0	-	-	-	-	-	42.1 $\pm$ 5.0	
V717 $\gamma$ 2	56.0 $\pm$ 22.0	-	-	-	-	-	-	65.0 $\pm$ 21.0	
V718 $\gamma$ 2	20.52 $\pm$ 0.32	-	18.9 $\pm$ 1.7	-	-	-	-	20.84 $\pm$ 0.83	15.13 $\pm$ 0.47
V723 $\gamma$ 1	16.76 $\pm$ 0.26	19.43 $\pm$ 0.62	15.45 $\pm$ 0.73	44.6 $\pm$ 2.3	34.6 $\pm$ 2.4	30.03 $\pm$ 0.71	17.42 $\pm$ 0.55	13.92 $\pm$ 0.15	
V723 $\gamma$ 2	18.52 $\pm$ 0.33	20.77 $\pm$ 0.96	20.3 $\pm$ 1.0	37.8 $\pm$ 3.3	36.8 $\pm$ 3.8	32.6 $\pm$ 1.2	18.94 $\pm$ 0.67	14.27 $\pm$ 0.37	
V729 $\gamma$ 1	49.5 $\pm$ 6.4	-	52.0 $\pm$ 10.0	-	-	77.0 $\pm$ 12.0	44.2 $\pm$ 10.0	32.4 $\pm$ 4.2	
V729 $\gamma$ 2	51.0 $\pm$ 12.0	-	-	-	-	-	-	49.0 $\pm$ 10.0	
V731 $\gamma$ 1	61.0 $\pm$ 16.0	-	-	-	-	-	-	41.7 $\pm$ 6.9	
L733 $\delta$ 1	31.9 $\pm$ 1.4	35.7 $\pm$ 7.3	30.7 $\pm$ 2.6	85.0 $\pm$ 14.0	39.0 $\pm$ 23.0	65.1 $\pm$ 4.5	32.9 $\pm$ 2.6	24.6 $\pm$ 1.7	
L733 $\delta$ 2	28.4 $\pm$ 1.1	36.3 $\pm$ 8.9	24.4 $\pm$ 2.8	64.0 $\pm$ 29.0	-	50.7 $\pm$ 5.4	32.4 $\pm$ 2.3	21.8 $\pm$ 1.0	
I738 $\delta$ 1	38.1 $\pm$ 1.5	46.2 $\pm$ 6.3	38.0 $\pm$ 2.4	-	-	63.7 $\pm$ 3.5	41.3 $\pm$ 2.1	35.0 $\pm$ 1.6	
I743 $\delta$ 1	25.29 $\pm$ 0.42	32.0 $\pm$ 2.0	22.2 $\pm$ 1.0	63.9 $\pm$ 3.9	50.0 $\pm$ 14.0	44.1 $\pm$ 1.5	25.07 $\pm$ 0.2	16.96 $\pm$ 0.33	
V745 $\gamma$ 1	31.5 $\pm$ 1.2	29.9 $\pm$ 4.2	31.8 $\pm$ 2.0	47.3 $\pm$ 9.8	-	45.5 $\pm$ 4.1	29.7 $\pm$ 1.8	22.6 $\pm$ 0.91	
I748 $\delta$ 1	20.32 $\pm$ 0.31	21.06 $\pm$ 0.79	22.9 $\pm$ 1.1	81.0 $\pm$ 18.0	33.1 $\pm$ 4.2	37.1 $\pm$ 1.4	21.06 $\pm$ 0.64	14.77 $\pm$ 0.33	

**Supplementary Table 4:** Methyl  $^1\text{H}$   $R_2$  measurements for RNCs.

Methyl	$S_{axis}^2 \tau_c(\text{ns})$								
	+67 950 MHz	+67 GS 950 MHz	+67 E6 950 MHz	+67 K2 950 MHz	+47 900 MHz	+57 900 MHz	+67 900 MHz	+110 900 MHz	
L661 $\delta$ 1	33.7 $\pm$ 4.8	31.0 $\pm$ 11.0	31.0 $\pm$ 8.1	-	-	66.0 $\pm$ 11.0	45.7 $\pm$ 7.6	32.9 $\pm$ 6.3	
L661 $\delta$ 2	63.7 $\pm$ 9.0	63.0 $\pm$ 18.0	74.0 $\pm$ 33.0	-	-	147.0 $\pm$ 33.0	65.0 $\pm$ 12.0	64.0 $\pm$ 13.0	
V664 $\gamma$ 1	13.63 $\pm$ 0.38	14.9 $\pm$ 1.4	14.59 $\pm$ 0.82	25.7 $\pm$ 3.8	28.7 $\pm$ 5.2	26.0 $\pm$ 1.6	15.62 $\pm$ 0.84	11.12 $\pm$ 0.41	
V664 $\gamma$ 2	12.8 $\pm$ 0.56	-	-	-	-	-	-	12.85 $\pm$ 0.66	
I674 $\delta$ 1	45.2 $\pm$ 3.7	42.3 $\pm$ 9.0	36.9 $\pm$ 5.5	-	-	53.1 $\pm$ 6.4	47.7 $\pm$ 4.8	31.3 $\pm$ 2.2	
V677 $\gamma$ 1	63.7 $\pm$ 5.1	72.0 $\pm$ 17.0	63.3 $\pm$ 5.6	-	-	95.0 $\pm$ 10.0	65.0 $\pm$ 11.0	57.2 $\pm$ 7.1	
V677 $\gamma$ 2	66.0 $\pm$ 11.0	-	51.0 $\pm$ 21.0	-	-	-	-	43.6 $\pm$ 9.2	
I695 $\delta$ 1	33.5 $\pm$ 2.3	42.7 $\pm$ 7.1	37.6 $\pm$ 5.2	116.0 $\pm$ 25.0	-	54.7 $\pm$ 5.3	34.7 $\pm$ 3.0	24.7 $\pm$ 1.6	
L701 $\delta$ 1	20.4 $\pm$ 1.9	19.2 $\pm$ 2.4	22.3 $\pm$ 3.5	80.0 $\pm$ 16.0	-	34.5 $\pm$ 3.6	19.9 $\pm$ 2.0	14.6 $\pm$ 1.0	
L701 $\delta$ 2	36.9 $\pm$ 5.0	40.0 $\pm$ 18.0	-	-	-	59.0 $\pm$ 12.0	35.8 $\pm$ 7.7	24.9 $\pm$ 2.9	
V702 $\gamma$ 1	40.7 $\pm$ 1.9	-	35.3 $\pm$ 2.0	-	54.2 $\pm$ 5.3	-	-	-	
V702 $\gamma$ 2	41.3 $\pm$ 1.8	41.8 $\pm$ 4.0	23.9 $\pm$ 2.6	133.0 $\pm$ 18.0	-	87.6 $\pm$ 5.0	62.9 $\pm$ 3.1	31.9 $\pm$ 1.9	
V703 $\gamma$ 1	48.6 $\pm$ 3.1	41.7 $\pm$ 7.7	40.8 $\pm$ 3.4	115.0 $\pm$ 28.0	-	62.0 $\pm$ 8.6	43.4 $\pm$ 5.2	32.9 $\pm$ 3.6	
V703 $\gamma$ 2	48.4 $\pm$ 6.8	47.0 $\pm$ 16.0	31.5 $\pm$ 3.8	-	-	73.0 $\pm$ 8.8	43.0 $\pm$ 10.0	29.7 $\pm$ 3.6	
V707 $\gamma$ 1	33.9 $\pm$ 2.2	33.8 $\pm$ 5.9	-	-	-	-	-	-	
V707 $\gamma$ 2	50.5 $\pm$ 5.9	37.0 $\pm$ 10.0	35.6 $\pm$ 4.1	-	-	-	-	-	
V717 $\gamma$ 1	48.1 $\pm$ 8.6	26.0 $\pm$ 21.0	-	-	-	-	-	41.7 $\pm$ 5.6	
V717 $\gamma$ 2	60.0 $\pm$ 25.0	-	-	-	-	-	-	72.0 $\pm$ 26.0	
V718 $\gamma$ 2	20.4 $\pm$ 1.1	-	18.6 $\pm$ 2.2	-	-	-	22.3 $\pm$ 1.3	15.16 $\pm$ 0.74	
V723 $\gamma$ 1	4.87 $\pm$ 0.29	5.64 $\pm$ 0.39	4.49 $\pm$ 0.33	12.9 $\pm$ 1.2	10.37 $\pm$ 0.95	9.02 $\pm$ 0.58	5.29 $\pm$ 0.31	4.25 $\pm$ 0.2	
V723 $\gamma$ 2	4.5 $\pm$ 0.13	5.1 $\pm$ 0.28	4.99 $\pm$ 0.3	9.64 $\pm$ 0.91	9.8 $\pm$ 1.1	8.64 $\pm$ 0.41	4.87 $\pm$ 0.22	3.58 $\pm$ 0.13	
V729 $\gamma$ 1	57.3 $\pm$ 8.1	-	61.0 $\pm$ 13.0	-	-	94.0 $\pm$ 16.0	52.0 $\pm$ 13.0	36.2 $\pm$ 5.6	
V729 $\gamma$ 2	64.0 $\pm$ 16.0	-	-	-	-	-	-	58.0 $\pm$ 13.0	
V731 $\gamma$ 1	48.0 $\pm$ 14.0	-	-	-	-	-	-	30.7 $\pm$ 6.4	
L733 $\delta$ 1	40.1 $\pm$ 2.7	46.0 $\pm$ 11.0	38.3 $\pm$ 4.2	118.0 $\pm$ 22.0	51.0 $\pm$ 34.0	90.2 $\pm$ 6.9	42.5 $\pm$ 3.9	30.3 $\pm$ 2.6	
L733 $\delta$ 2	18.0 $\pm$ 1.0	24.3 $\pm$ 7.2	14.8 $\pm$ 2.3	46.0 $\pm$ 23.0	-	36.8 $\pm$ 4.4	22.3 $\pm$ 1.9	13.76 $\pm$ 0.83	
I738 $\delta$ 1	42.7 $\pm$ 2.1	52.6 $\pm$ 7.8	42.6 $\pm$ 3.1	-	-	76.7 $\pm$ 4.8	47.9 $\pm$ 2.9	39.8 $\pm$ 2.2	
I743 $\delta$ 1	28.84 $\pm$ 0.77	37.1 $\pm$ 2.6	25.1 $\pm$ 1.3	76.5 $\pm$ 5.1	62.0 $\pm$ 18.0	53.7 $\pm$ 2.3	29.28 $\pm$ 0.7	18.88 $\pm$ 0.54	
V745 $\gamma$ 1	20.8 $\pm$ 1.1	19.7 $\pm$ 3.2	21.1 $\pm$ 1.6	32.6 $\pm$ 7.3	-	33.3 $\pm$ 3.6	20.6 $\pm$ 1.7	14.89 $\pm$ 0.91	
I748 $\delta$ 1	27.2 $\pm$ 1.9	28.2 $\pm$ 2.2	30.9 $\pm$ 2.7	112.0 $\pm$ 27.0	48.4 $\pm$ 6.9	54.5 $\pm$ 3.5	29.9 $\pm$ 1.6	20.19 $\pm$ 0.85	

**Supplementary Table 5:** Calculated methyl  $S_{axis}^2 \tau_c$  values for RNCs.

## References

1. Hsu, S.-T. D., Cabrita, L. D., Fucini, P., Christodoulou, J. & Dobson, C. M. Probing side-chain dynamics of a ribosome-bound nascent chain using methyl NMR spectroscopy. *J. Am. Chem. Soc.* **131**, 8366–8367 (2009).